

## Electronic Supplementary Information

# Multifunctional Nanoarchitected Porous Carbon for Solar Steam Generation and Supercapacitor Applications

*Nitish Kumar,<sup>a</sup> Tawseef Ahmad Wani,<sup>a</sup> Prakash Kumar Pathak<sup>a</sup> Ashok Bera,<sup>a,\*</sup> and Rahul R. Salunkhe<sup>a,\*</sup>*

Department of Physics, Indian Institute of Technology, Jammu, J&K, India (181221).

## Note S1

We have used the following equations<sup>1</sup> for calculating specific capacitance (SC), specific energy (SE), and specific power (SP).

### ***CV calculations:***

SC calculations from CV measurements were calculated as,

$$\text{SC} = \frac{1}{ms(V_f - V_i)} \int_{V_i}^{V_f} I(V) dV \quad (\text{S1})$$

Where ‘m’ is active mass loading, ‘s’ is the scan rate ( $\text{mV s}^{-1}$ ), “ $V_i$ ” is the Initial potential, “ $V_f$ ” is the final potential,  $I(V)$  is the response current density from the CV curve.

### ***GCD calculations:***

GCD calculations for two-electrode cells were calculated using the following equations:

$$\text{SC (F g}^{-1}\text{)} = \frac{(I \times \Delta t)}{M \times (V_f - V_i)} \quad (\text{S2})$$

$$\text{SE (Wh kg}^{-1}\text{)} = \frac{\frac{1}{2}C_s V^2}{3.6} \quad (\text{S3})$$

$$\text{SP (KW kg}^{-1}\text{)} = \frac{3600 \times SE}{\Delta t} \quad (\text{S4})$$

Where “ $I$ ” is the charge/discharge current at time  $t(s)$ , “ $\Delta t$ ” is the discharge time, “ $\Delta V$ ” is the voltage window

“ $M$ ” is the total active mass on both electrodes (i.e  $M = 2m$ ,  $m$  is the active mass loading on single electrode).

### ***Solar absorbance calculation:***

The percentage solar absorbance ( $\alpha$ ) is calculated by using the equation

$$\alpha = \frac{\int_{300}^{2500} (1 - R(\lambda))I(\lambda)}{\int_{300}^{2500} I(\lambda)} \times 100 \quad (\text{S5})$$

where  $\lambda$  is the wavelength,  $I(\lambda)$  is the light intensity function of the solar spectrum, and  $R(\lambda)$  is the reflectivity function of the sample at different  $\lambda$ .

***Evaporation efficiency:***

The evaporation efficiency ( $\eta$ ) was calculated by using the following equation:

$$\eta = \frac{\dot{m}h_{LV}}{q_i} \quad (\text{S6})$$

where  $\dot{m}$  is the evaporation rate,  $h_{LV}$  is the evaporation enthalpy, and  $q_i$  is the total solar intensity.

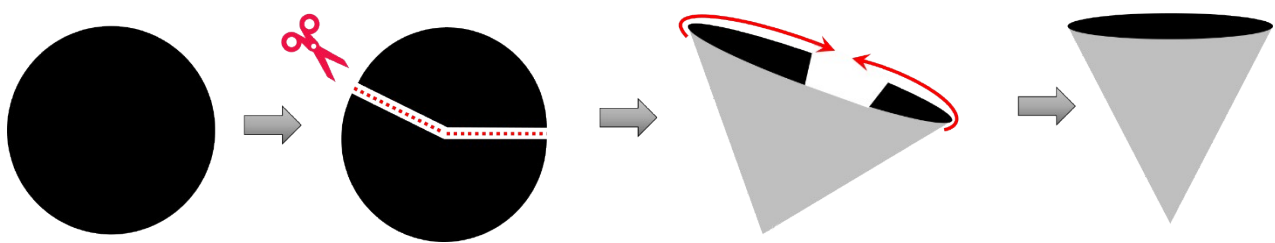


**Fig. S1.** Stepwise process for the conversion of the 2D sheet to the 3D cone for further utilization in SSG application.

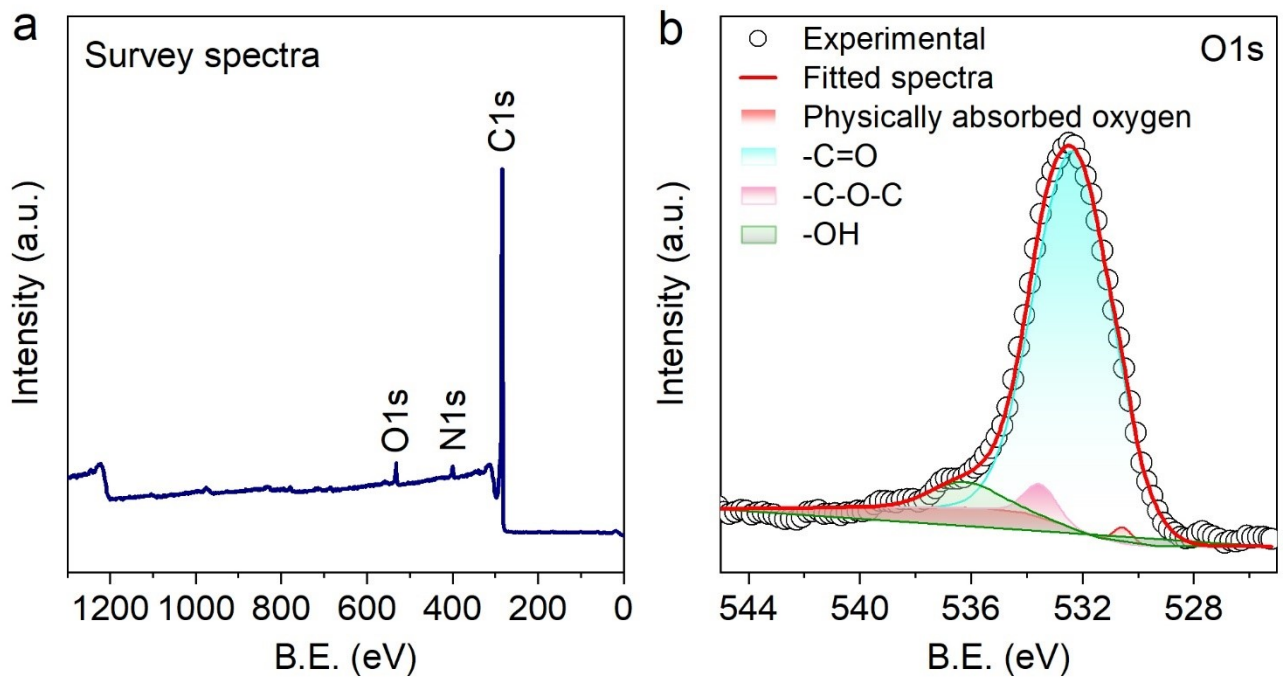


**Fig. S2.** (a) XPS survey spectra for NPC showing the presence of carbon, nitrogen, and oxygen. (b) The high-resolution narrow region spectra of O 1s.

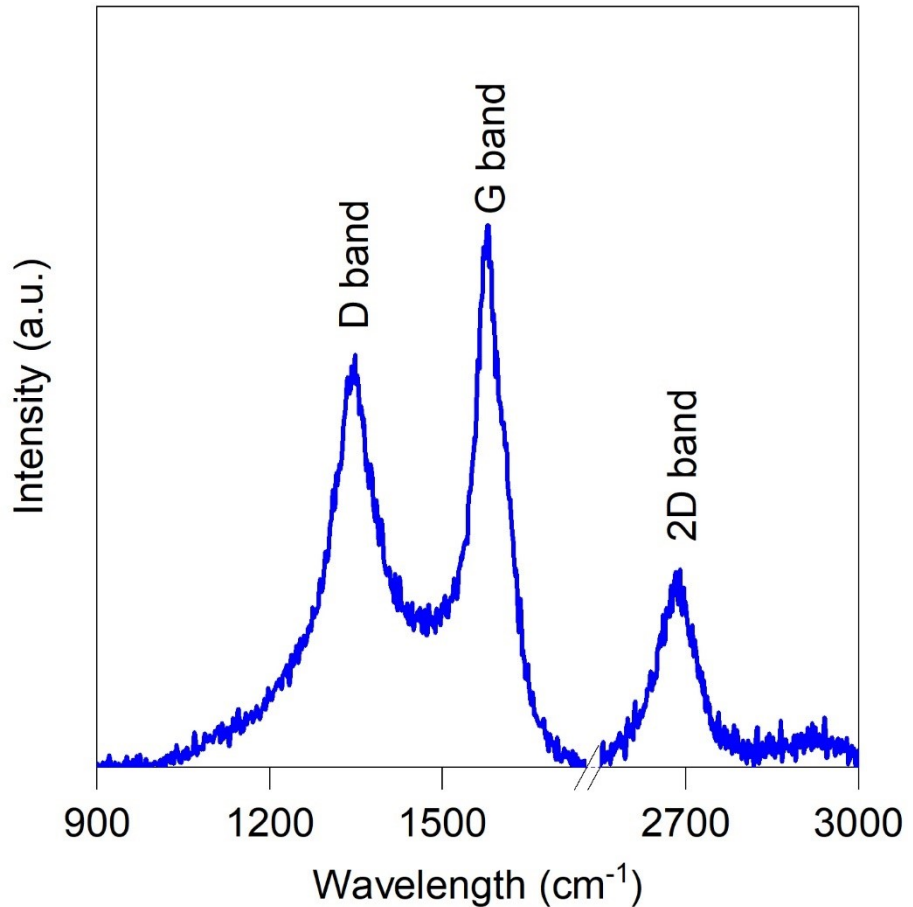


**Fig. S3.** Raman spectra for NPC show the presence of D, G, and 2D bands

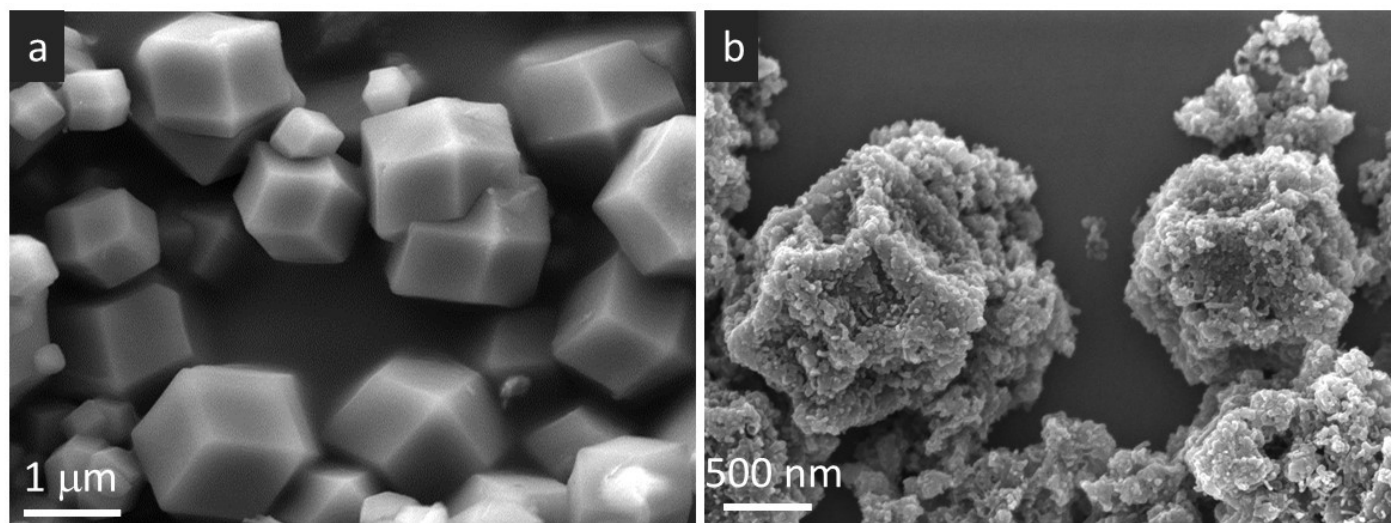


**Fig. S4.** FESEM images before and after carbonization. (a) ZIF-67 polyhedron particles before carbonization, and (b) NPC particles retaining polyhedron shape after carbonization and HF washing.

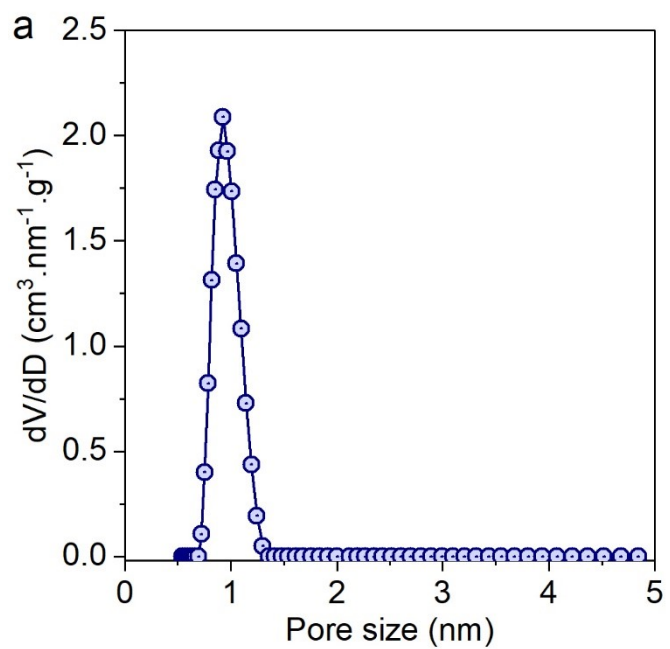


**Fig. S5.** DFT model predicted pore size distribution for ZIF-67 sample, showing the presence of micropores (~0.92 nm).

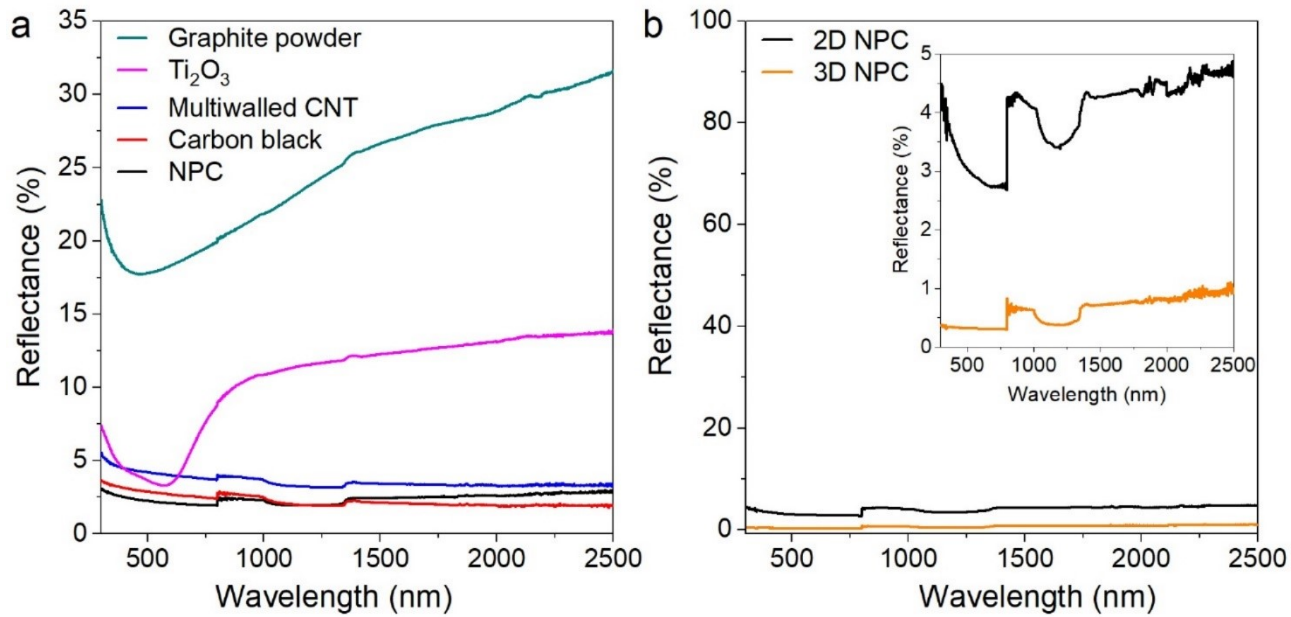


**Fig. S6.** (a) Comparison for the absorption of our NPC sample with  $\text{Ti}_2\text{O}_3$  and other carbon-based materials, indicating the superiority of NPC over other materials. (b) The diffuse reflectance of NPC-67 in 2D and 3D cone-shaped configurations.

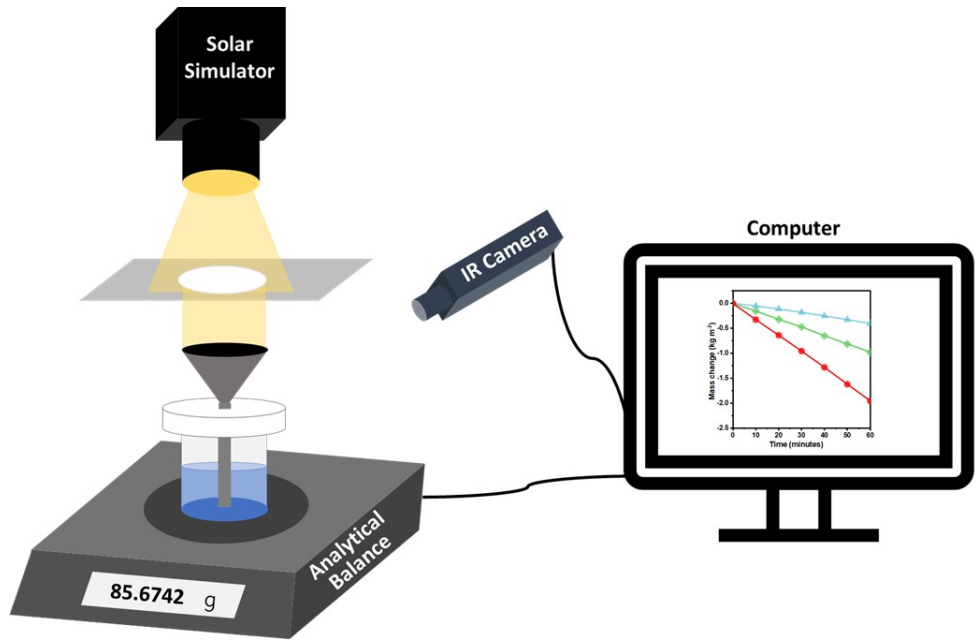


**Fig. S7.** Schematic experimental setup for evaluation of evaporation performance.

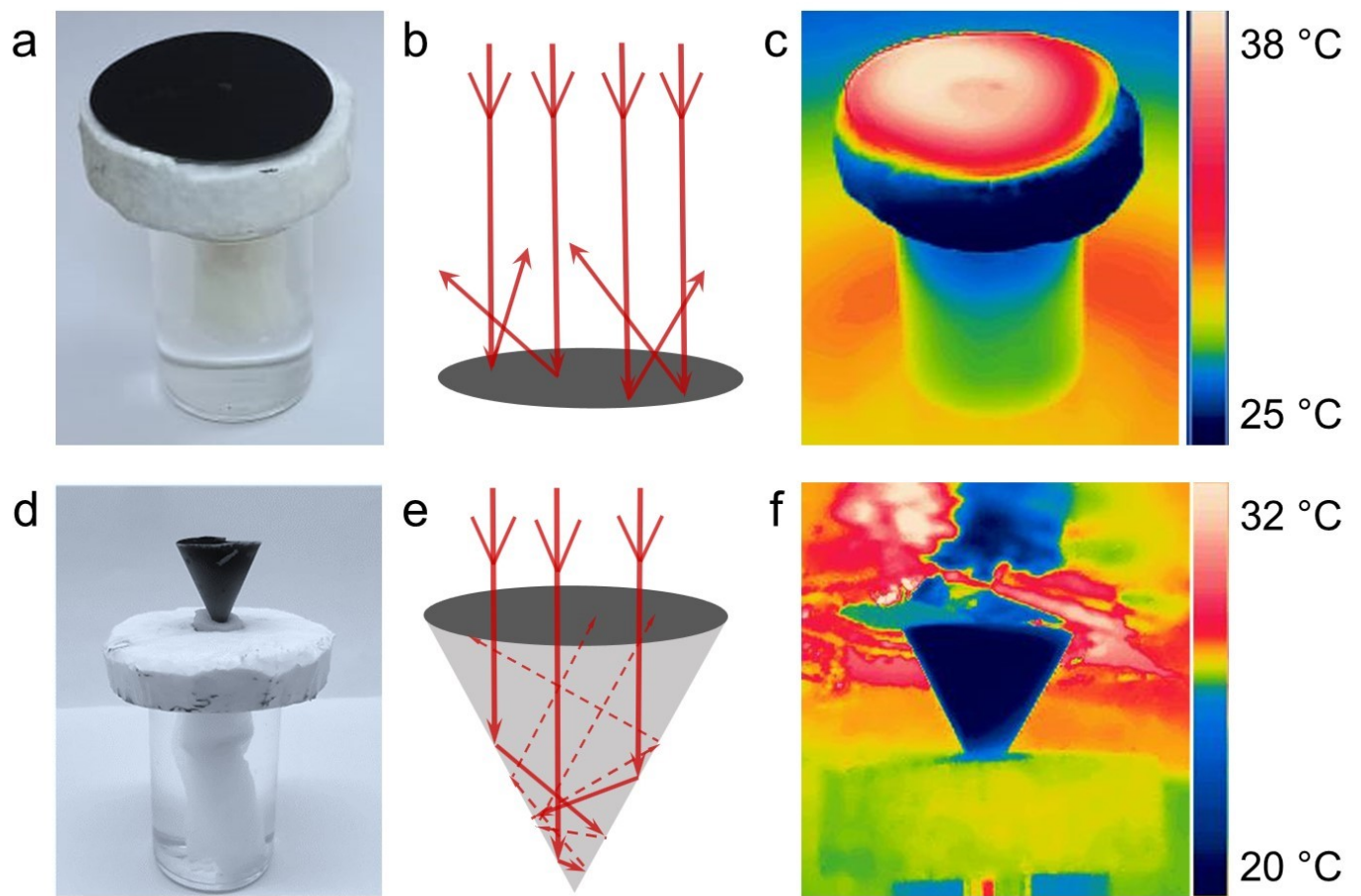


**Fig. S8.** Digital photographs and concept visualizations for 2D and 3D cone-shaped evaporators. Actual photograph of the 2D disk (a) and 3D cone-shaped evaporator (d). The ray diagram of 2D (b) and 3D (e) evaporator demonstrates the advantage of 3D cone shape over disk evaporator, showing that the cone walls efficiently recycle diffuse reflection light. IR thermal images under 1 sun illumination demonstrate the energy loss in 2D (c) and gain in 3D (f) evaporators due to the temperature difference in the evaporator and ambient atmosphere.



**Fig. S9.** Actual photograph of pH meter readings and inset showing Litmus paper test results. The pH value of (a) acidic solution before purification, (b) alkaline solution before purification, and (c) purified water after SSG

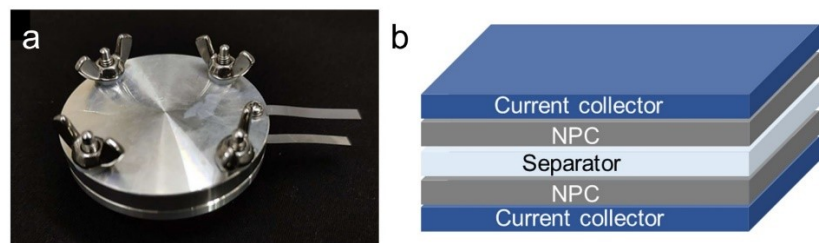


**Fig. S10.** (a) Actual picture of HS Flat cell used for two-electrode measurements. (b) Arrangement of electrodes inside the packed device.

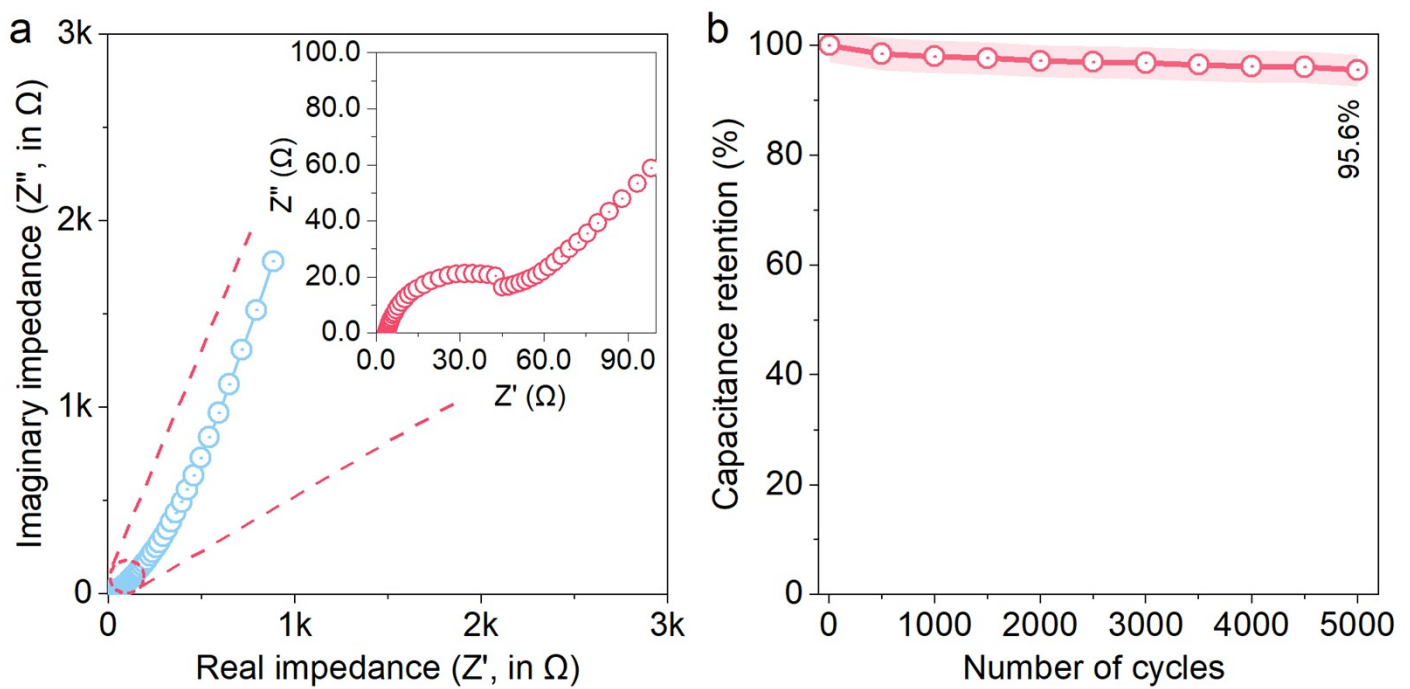


**Fig. S11.** (a) Nyquist plot showing the real impedance *vs.* imaginary impedance for the packed device in [emim][BF<sub>4</sub>]/PC electrolyte, and (b) cyclic stability test for the NPC device at a current density of 5 A g<sup>-1</sup>.

**Table S1.** SSG performance comparison with the previous literature reports.

S.N.	Materials	Solar intensity	Evaporation rate (kg m <sup>-2</sup> h <sup>-1</sup> )	Reference
1	Carbon particles on air laid paper	1	0.964	2
2	Black titania/graphene oxide nanocomposite film on air-laid paper and polyethylene foam	1	1.2	3
3	Patterned surfaces by printing carbon black on air-laid paper	1	1	4
4	Carbon nanotube membrane on a macroporous silica substrate	1	1.25	5
5	Functionalized graphene	1	0.52	6
6	rGO/mixed cellulose esters	1	0.9	7
7	Thin coating of CNTs on the top surface of a tree stump with roots	10	12	8
8	Janus absorber (CB, PMMA and PAN)	1	1.3	9
9	Flame-treated wood	1	1.05	10
10	Black PAN/CB membrane on a green leaf	0.3	0.21	11
11	Activated carbon fiber felt	1	1.22	12
12	MOF derived porous carbon	1	1.22	13
13	MOF based hierarchical structure	1	1.5	14
14	Mn-MOF nanoflowers	1	1.31	15
15	Fe-MOF-74-based flexible composite	1	1.35	16
16	Cu-MOF textile	1	1.52	17
17	NPC- 67 planar (2D)	1	1.4	
18	NPC-67 cone-shaped	1	2.1	This work

**Table S2.** Three-electrode performance comparison of our NPC with previous literature reports.

S.N.	Materials	Electrolyte	Mass loading (mg)	Voltage window (V)	Scan rate (mV s <sup>-1</sup> )	Capacitance (F g <sup>-1</sup> )	Reference
1	Carbon derived from pyridine	1M H <sub>2</sub> SO <sub>4</sub>	-	0.5	1	182	18
2	Carbon foam	1M H <sub>2</sub> SO <sub>4</sub>	-	0.4	1	228	19
3	Porous carbon nanofiber	6M KOH	-	1	-	119	20
4	ZIF-8 derived carbon	1M H <sub>2</sub> SO <sub>4</sub>	1	0.9	5	251	21
5	DUT-5 derived carbon	6M KOH	3	0.5	-	119	22
6	MOF derived carbon nanosheets	6M KOH	-	1	-	283	23
7	MOF-derived carbon	6M KOH	1	1	-	212	24
8	Co/Zn-ZIF-derived NPC	0.5M H <sub>2</sub> SO <sub>4</sub>	-	0.8	-	286	25
9	MOF-5 derived carbon nano-spheres	6M KOH	-	1	2	193	26
10	MOF derived porous carbon	6M KOH	4-5	0.8	-	230	27
11	Hierarchical porous carbon	1M H <sub>2</sub> SO <sub>4</sub>	-	1.1	5	214	28
12	NPC	6M KOH	0.5	0.8	5	299.3	This work

**Table S3.** Specific energy and specific power values at different current densities for NPC two-electrode device.

S.N.	Current density ( $\text{A g}^{-1}$ )	Specific energy ( $\text{Wh kg}^{-1}$ )	Specific power ( $\text{W kg}^{-1}$ )
1	0.1	16.9	242.1
2	0.2	15.5	468.5
3	0.3	14.5	679.7
4	0.4	13.4	876.1
5	0.5	13.2	1113.9
6	0.6	12.5	1314.2
7	0.7	11.9	1507.1
8	0.8	10.9	1678.1
9	0.9	10.3	1855
10	1	9.7	2025
11	3	7.3	4896.5
12	5	5.5	6480
13	7	5.1	9173.1
14	10	3.8	10890

## References

- 1 G. Eda, G. Fanchini and M. Chhowalla, *Nat. Nanotechnol.*, 2008, **3**, 270–274.
- 2 S. Liu, C. Huang, X. Luo and Z. Rao, *Appl. Therm. Eng.*, 2018, **142**, 566–572.
- 3 X. Liu, B. Hou, G. Wang, Z. Cui, X. Zhu and X. Wang, *J. Mater. Res.*, 2018, **33**, 674–684.
- 4 Y. Luo, B. Fu, Q. Shen, W. Hao, J. Xu, M. Min, Y. Liu, S. An, C. Song, P. Tao, J. Wu, W. Shang and T. Deng, *ACS Appl. Mater. Interfaces*, 2019, **11**, 7584–7590.
- 5 Y. Wang, L. Zhang and P. Wang, *ACS Sustain. Chem. Eng.*, 2016, **4**, 1223–1230.
- 6 J. Yang, Y. Pang, W. Huang, S. K. Shaw, J. Schiffbauer, M. A. Pillers, X. Mu, S. Luo, T. Zhang, Y. Huang, G. Li, S. Ptasinska, M. Lieberman and T. Luo, *ACS Nano*, 2017, **11**, 5510–5518.
- 7 G. Wang, Y. Fu, X. Ma, W. Pi, D. Liu and X. Wang, *Carbon*, 2017, **114**, 117–124.
- 8 Y. Wang, H. Liu, C. Chen, Y. Kuang, J. Song, H. Xie, C. Jia, S. Kronthal, X. Xu, S. He and L. Hu, *Adv. Sustain. Syst.*, 2019, **3**, 1800055.
- 9 W. Xu, X. Hu, S. Zhuang, Y. Wang, X. Li, L. Zhou, S. Zhu and J. Zhu, *Adv. Energy Mater.*, 2018, **8**, 1702884.
- 10 G. Xue, K. Liu, Q. Chen, P. Yang, J. Li, T. Ding, J. Duan, B. Qi and J. Zhou, *ACS Appl. Mater. Interfaces*, 2017, **9**, 15052–15057.
- 11 S. Zhuang, L. Zhou, W. Xu, N. Xu, X. Hu, X. Li, G. Lv, Q. Zheng, S. Zhu, Z. Wang and J. Zhu, *Adv. Sci.*, 2018, **5**, 1700497.
- 12 H. Li, Y. He, Y. Hu and X. Wang, *ACS Appl. Mater. Interfaces*, 2018, **10**, 9362–9368.
- 13 S. Ma, W. Qarony, M. I. Hossain, C. T. Yip and Y. H. Tsang, *Sol. Energy Mater. Sol. Cells*, 2019, **196**, 36–42.
- 14 Q. Ma, P. Yin, M. Zhao, Z. Luo, Y. Huang, Q. He, Y. Yu, Z. Liu, Z. Hu, B. Chen and H. Zhang, *Adv. Mater.*, 2019, **31**, 1808249.
- 15 J. Wang, W. Wang, X. Mu, Z. Li and C. Wang, *Sustain. Energy Fuels*, 2021, **5**, 1995–2002.
- 16 J. Wang, W. Wang, J. Li, X. Mu, X. Yan, Z. Wang, J. Su, T. Lei and C. Wang, *ACS Appl. Mater. Interfaces*, 2021, **13**, 45944–45956.
- 17 J. Wang, W. Wang, L. Feng, J. Yang, W. Li, J. Shi, T. Lei and C. Wang, *Sol. Energy Mater. Sol. Cells*, 2021, **231**, 111329.
- 18 M. Kodama, J. Yamashita, Y. Soneda, H. Hatori, S. Nishimura and K. Kamegawa, *Mater. Sci. Eng. B*, 2004, **108**, 156–161.
- 19 M. Kodama, J. Yamashita, Y. Soneda, H. Hatori and K. Kamegawa, *Carbon*, 2007, **45**, 1105–1107.
- 20 P. Li, X. Ma, F. Liu, Y. L. Zhao, Y. Ding and J. Yang, *Microporous Mesoporous Mater.*, 2020, **305**, 110283.
- 21 R. R. Salunkhe, Y. Kamachi, N. L. Torad, S. M. Hwang, Z. Sun, S. X. Dou, J. H. Kim and Y. Yamauchi, *J. Mater. Chem. A*, 2014, **2**, 19848–19854.
- 22 Y. Liu, J. Xu and S. Liu, *Microporous Mesoporous Mater.*, 2016, **236**, 94–99.
- 23 K. Zhao, S. Liu, G. Ye, Q. Gan, Z. Zhou and Z. He, *J. Mater. Chem. A*, 2018, **6**, 2166–2175.
- 24 X. Deng, J. Li, S. Zhu, L. Ma and N. Zhao, *Energy Storage Mater.*, 2019, **23**, 491–498.
- 25 J. Kim, C. Young, J. Lee, M. S. Park, M. Shahabuddin, Y. Yamauchi and J. H. Kim, *Chem. Commun.*, 2016, **52**, 13016–13019.
- 26 I. A. Khan, A. Badshah, I. Khan, D. Zhao and M. A. Nadeem, *Microporous Mesoporous Mater.*, 2017, **253**, 169–176.
- 27 Y. Pan, Y. Zhao, S. Mu, Y. Wang, C. Jiang, Q. Liu, Q. Fang, M. Xue and S. Qiu, *J. Mater. Chem. A*, 2017, **5**, 9544–9552.
- 28 Q. Li, Z. Dai, J. Wu, W. Liu, T. Di, R. Jiang, X. Zheng, W. Wang, X. Ji, P. Li, Z. Xu, X. Qu, Z. Xu and J. Zhou, *Adv. Energy Mater.*, 2020, **10**, 1903750.